BNL-224169-2023-TECH
EIC-ADD-TN-043

# A numerical evaluation of the ambient air temperature in the Electron-Ion Collider tunnel

E. Letourneau, R. Srinivasan

August 2022

Electron-Ion Collider

**Brookhaven National Laboratory**

**U.S. Department of Energy**

USDOE Office of Science (SC), Nuclear Physics (NP) (SC-26)

# DISCLAIMER

A numerical evaluation of the ambient air temperature in the Electron-Ion Collider tunnel

Emma Letourneau
Department of Mechanical Engineering, University of Nevada Las Vegas, Las Vegas, NV 89154

Ram Srinivasan
Electron-Ion Collider Infrastructure Department, Brookhaven National Laboratory, Upton, NY, 11973

**Abstract**

The Electron-Ion Collider (EIC) is a next-generation collider-accelerator that may require consistent operating temperature conditions for the beams within the accelerator tunnels to maintain stable operation. Variations in ambient temperature within the tunnel can cause thermal expansion of beampipe and component supports and can negatively affect the tunnel equipment, impacting the stability of the beamline. Modifications will be made to the Relativistic Heavy Ion Collider (RHIC) at Brookhaven National Laboratory (BNL) to create the EIC, which necessitates a temperature model that addresses these modifications. To approach this problem, the consistency of temperature changes in different tunnel sections was first evaluated by plotting RHIC tunnel temperature data at various times of the day and year. From this data, a tunnel section was selected and a 2D temperature model was created for RHIC, EIC, and EIC with added cooling configurations. Soil temperature data was analyzed to determine the maximum, average, and mode soil temperatures, which were used as boundary conditions in different temperature scenarios. Computational fluid dynamics modeling was used to create 2D temperature profiles for the configurations. From this model, the predicted temperatures indicate that further analysis is required to validate the boundary conditions and benchmark the current conditions to allow the prediction of the tunnel ambient conditions at EIC. This research can be used as a preliminary model to create an EIC tunnel cooling system that will increase the operational stability of the EIC. As a result of my work this summer, I have become familiar with computational fluid dynamics, including creating fluid dynamic simulations using ANSYS Fluent and related software. I have also learned about the project process required for planning large-scale engineering projects.

## Introduction

Brookhaven National Laboratory (BNL) is currently host to the Relativistic Heavy-Ion Collider (RHIC), an accelerator-collider that uses heavy ions to study the inner structure of the nucleon. While RHIC has been an essential instrument of discovery for over two decades, the collision of heavy ions creates extraneous data that limits discoveries of the inner nature of the nucleon. This limitation will be addressed through the Electron-Ion Collider (EIC), an upgrade to RHIC that replaces a heavy ion beam with an electron beam. With this upgrade physicists can examine the inner nature of the atom and its components in greater detail, supporting decades of future scientific discoveries and innovations.

The EIC requires great precision in factors such as beam crossing locations and sensor conditions to maintain stable operation. Thermal expansion from temperature changes can impact the EIC's beam supports, while changing temperatures can alter sensor functionality. Additional components and heat loads make the tunnel layout of the EIC substantially different from RHIC, so past operational stability and temperature data for RHIC cannot predict future EIC operation. For this reason, predicting the temperature profile of the EIC tunnel is essential to the accelerator-collider's success.

This paper focuses on creating a 2D temperature model of a representative section of the EIC tunnel by numerically solving natural convection through the mass, momentum, and energy conservation equations with buoyancy effects. This model only considers the more-common curved metal section of the RHIC tunnels and does not consider the less-common concrete tunnel sections. The model incorporates the major RHIC components as well as the components that will be added to the EIC: the Rapid Cycling Synchrotron (RCS), the Electron Storage Beam

(ESR), and two additional water pipes. Creating this model will provide a tool to further analyze and evaluate the necessity of an air-cooling system for the EIC.

## Methods

This model was evaluated using computational fluid dynamics (CFD) through Ansys Fluent and related tools. To create the model and define the computational parameters, a few assumptions were made. The tunnel shape and internal components were assumed constant over all tunnel sections, and it was assumed that there was no horizontal natural convection or changes in the heat sources through the tunnel. These assumptions allowed for a 2D model to be used in place of a 3D model. Complex geometries were simplified to their base shapes to reduce unnecessary complexity and model run time.[1] These simplifications are not expected to have significant impacts on the results. The tunnel structure is made of a circular corrugated steel sheet buried under layers of soil, the depth of which varies throughout the ring. This corrugation was simplified to a flat surface, and with a 16-foot diameter used as a representative portion of the tunnel for this model[2]. Additional dimensions for the RHIC components and tunnel structure were taken from AutoCAD drawings[3] and dimensions for the EIC elements were taken from EIC Creo Drawings[4] both pictured in Figure 1.

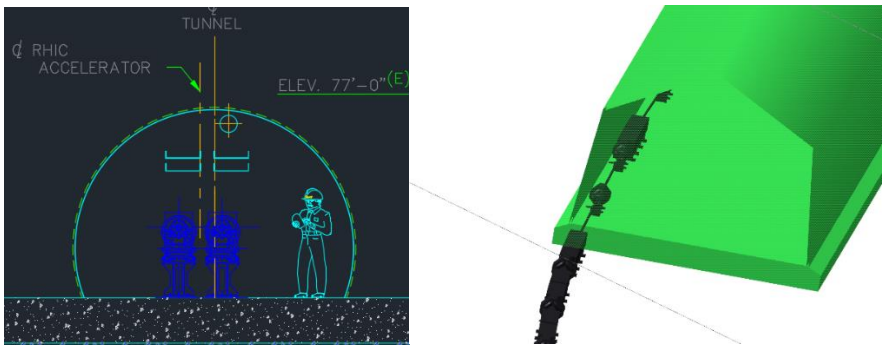


**Figure 1: AutoCAD drawing of RHIC tunnel (left) and Creo snapshot of RCS in EIC tunnel (right)**

These elements were used to create the model drawing shown in Figure 2. The soil was assumed to be an infinite heat source[5,6] and modeled as a six-inch layer surrounding the tunnel.

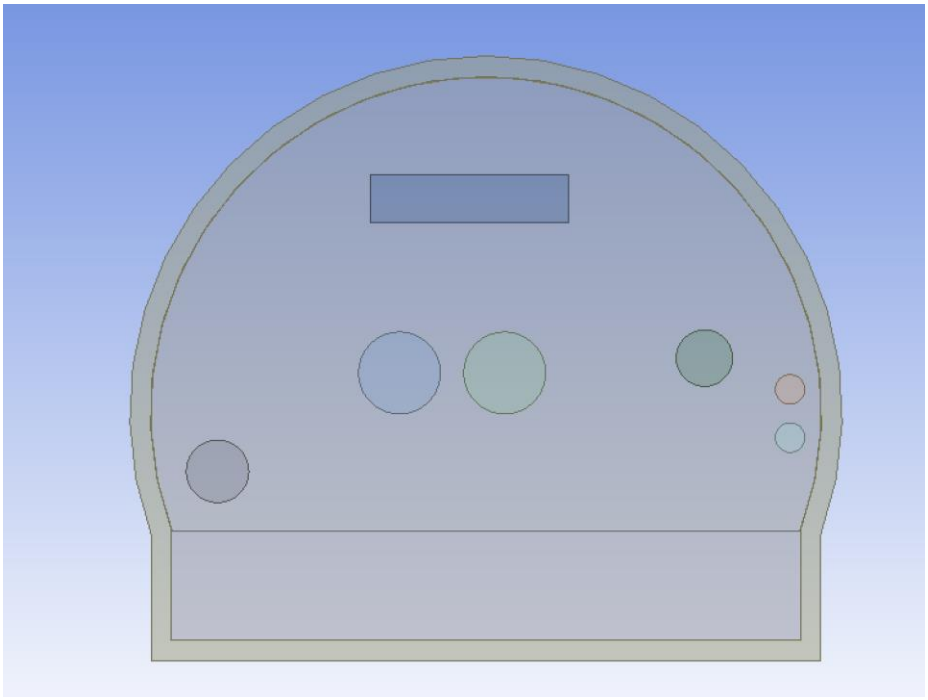

**Figure 2: 2D model of EIC tunnel**

The elements included in the model (Figure 2) from left to right include the Rapid Cycling Synchrotron (RCS), two central Hadron beams, the cable tray, the Electron Storage Ring (ESR), and two 8" diameter water pipes. The cable tray was considered as one lumped heat source, eliminating the need to determine heat losses for individual conductors. Meshing was considered acceptable when the skewness was less than 0.95 for all elements and the orthogonal quality was over 0.15 for all elements. This goal was reached with most components being reasonably close to or at zero for skewness and one for orthogonal quality.

To create the boundary conditions for the different tunnel configurations, the temperatures and heat generation of each element was evaluated for each configuration. Since this model is 2D, heat generation elements were considered for a one meter depth of tunnel section, which is a built-in feature of heat generation included in 2D Ansys Fluent modeling. The

Hadron Beams contain magnets that are cooled by circulating supercritical helium surrounded by an insulating jacket, which results in heat sinks with negative heat values. The heat generation rate and associated calculation are shown in Table 1.

**Table 1: Calculated Boundary Conditions**

| | Heat values $(W/m)$ | Cross-Sectional Surface Area $(m^2)$ | Heat Generation Rate $(W/m^3)$ |
|---|---|---|---|
| RCS[7] | 93.333 | 0.170232 | 548.269 |
| Cable Tray[8] | 99.72 | 0.523870 | 190.353 |
| Hadron Beams (combined)[9] | -3.5 | 0.291864 | -11.9919 |

Other boundary conditions include constant temperature values assigned to figure walls. The upper water pipe was assigned a temperature of 96°F, while the lower water pipe was assigned a temperature of 86°F. These boundary conditions were determined by assuming the pipe wall temperature is equal to the target fluid temperature of the pipe water, which remains constant. In reality these wall temperatures would be lower due to heat losses through the pipe walls, but these values were considered appropriate bounding temperatures as they are conservative. Soil temperature values were calculated based on a depth of six inches from March through June[10]. The outer wall of the soil wall was assigned either the maximum soil temperature of 83°F, the average soil temperature of 59°F, or the mode soil temperature of 53°F. It was assumed that a six-inch soil depth would accurately represent the temperature of the soil surrounding RHIC. The ESR was assigned no boundary conditions. Density, thermal conductivity, and specific heat values for steel and aluminum were taken from Ansys Fluent's database, and for concrete and dirt were taken from *Heat and Mass Transfer: Fundamentals & Applications, 4th Edition.*[11]

Five configurations were run at each of these temperatures. The first was the RHIC configuration in operation, which used the RHIC layout with operational heat sources. This

configuration included heat generation from cable tray and the Hadron Beams. The second was the RHIC configuration while dormant (RHIC-D), which used the RHIC layout without operational heat sources. The third configuration used the EIC's proposed layout while operational, which included all heat generation elements and water pipes except one Hadron Beam, as this beamline is not in operation in EIC models. The fourth configuration used the EIC layout with an additional cooling pipe added (EIC-C1), while the fifth configuration included two cooling pipes (EIC-C2). These eight-inch diameter cooling pipes were added to the top right and left corners, and were assigned constant wall temperatures of 45°F.

Convergence for the models was determined using the total heat transfer rate option of the flux reports feature built into Ansys Fluent. The model was considered converged if the net heat transfer was less than or equal to five percent of the user-defined heat transfer. The exception was the RHIC-D model, which had no heat transfer values. This model was considered converged when the residuals reached below 0.001.

## Results

### *Analysis of RHIC Data to Determine Model Characteristics*

The first step in the modeling process was to determine whether a singular model could be a reasonable representation of all the steel-walled sections of the tunnel, regardless of time of day or year. Time of day was considered through plotting the RHIC tunnel temperature data[9] for the entire ring at four times of the day. For both March 14$^{th}$ and June 12$^{th}$, the temperature pattern stayed reasonably consistent throughout the day, suggesting that the model can assume that time of day is inconsequential. These graphs are shown in Figure 3.

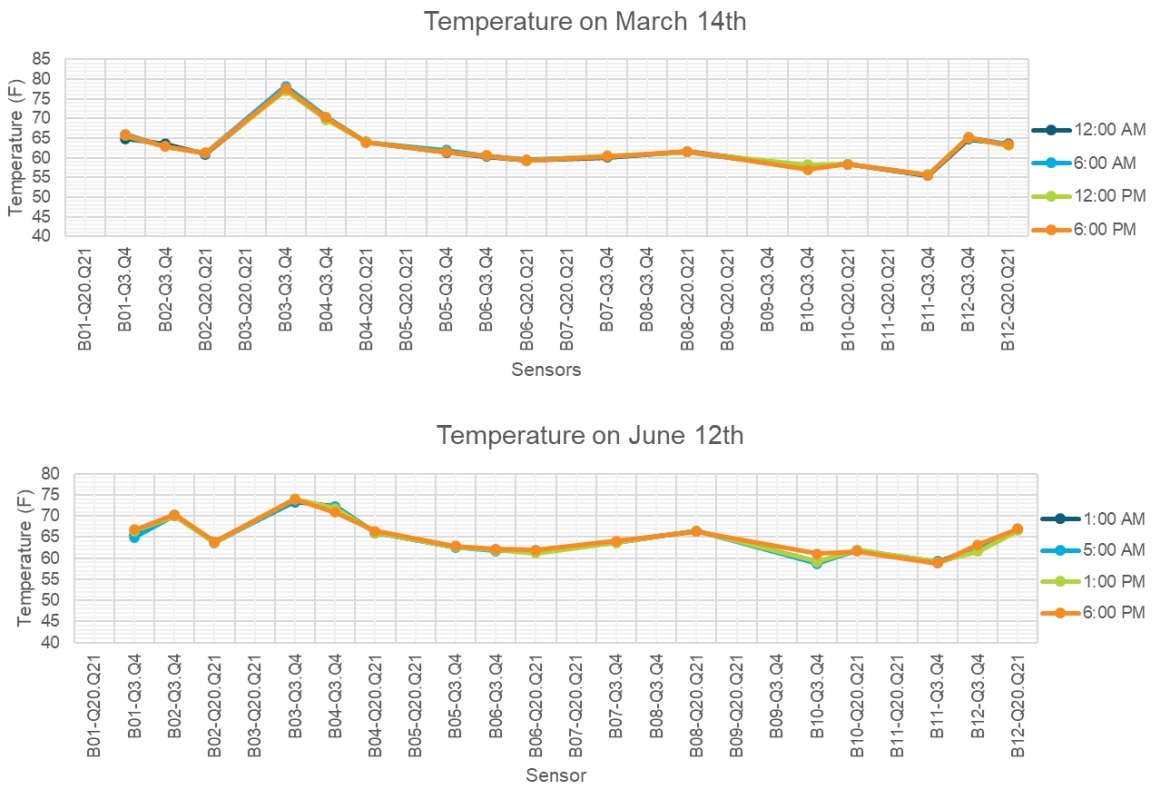


**Figure 3: Plots of all RHIC sensors during four different times of day, plotted in separate graphs for two different days**

The impact of outdoor ambient temperature on tunnel temperatures was then examined by graphing both the outdoor ambient temperature[12] and three tunnel sensor temperatures for three times of the year. These graphs, shown in Figure 4, revealed that variations in the outdoor ambient temperature throughout the day had no impact on the daily sensor temperature, but that both outdoor ambient temperature and tunnel sensor temperature varied during the year. This suggests that outdoor ambient temperature does not directly impact daily tunnel temperatures but may impact the tunnel temperature throughout the year. The most likely source of this impact is through the warming and cooling of the soil layer that covers RHIC. These results mean that the model does not need to consider the time of day but should be run at different soil temperatures to account for temperature differences throughout the year.

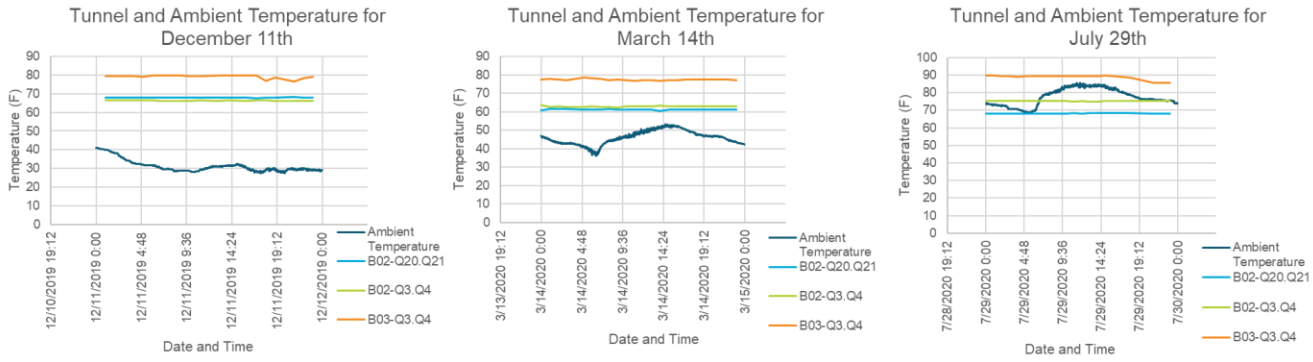


**Figure 4: Three sensor temperatures and the ambient temperature plotted through the day for three days of the year**

*Simulation Results*

The model was run for a steady state solution until convergence was reached for each soil temperature and model configuration combination. Table 2 shows the number of iterations run for each model, as well was the resulting test for convergence.

**Table 2: Convergence Data**

| Model Configuration | Soil Temperature (°F) | Iterations | Percent Net Convergence of User-Defined Heat Transfer (%) |
|---|---|---|---|
| RHIC | 83 | 10000 | 4.696 |
| | 59 | 10000 | 4.929 |
| | 53 | 10000 | 0.527 |
| RHIC-D | 83 | 164 | N/A |
| | 59 | 228 | N/A |
| | 53 | 218 | N/A |
| EIC | 83 | 5000 | 4.766 |
| | 59 | 5000 | 4.054 |
| | 53 | 5000 | 5.001 |
| EIC-C1 | 83 | 4000 | 3.370 |
| | 59 | 5000 | 1.186 |
| | 53 | 5000 | 1.338 |
| EIC-C2 | 83 | 10000 | 0.272 |
| | 59 | 10000 | 0.571 |
| | 53 | 10000 | 0.188 |

Figure 6 shows the global temperature profile for the RHIC configuration of the model using the maximum soil temperature, average soil temperature, and mode soil temperature. Additionally, a graph of the temperature distribution of the model, taken from a vertical line through the midpoint of the figure is shown to the right of each image. The area of interest in these graphs is shown by the blue box. This area of interest extends from slightly above the tunnel floor to slightly below the cable rack and represents where temperature would be most impactful on the EIC's beams and sensors. To define the boundaries of the area of interest, the x-axis values of -30.0 to 50.0 were used, where zero is the exact center of the tunnel if drawn as a perfect circle. An example of the locations of the tunnel floor and the bottom of the cable tray can be seen in Figure 5. Note that the peak on the graph in this paper represents the cable tray and is not representative of air temperature.

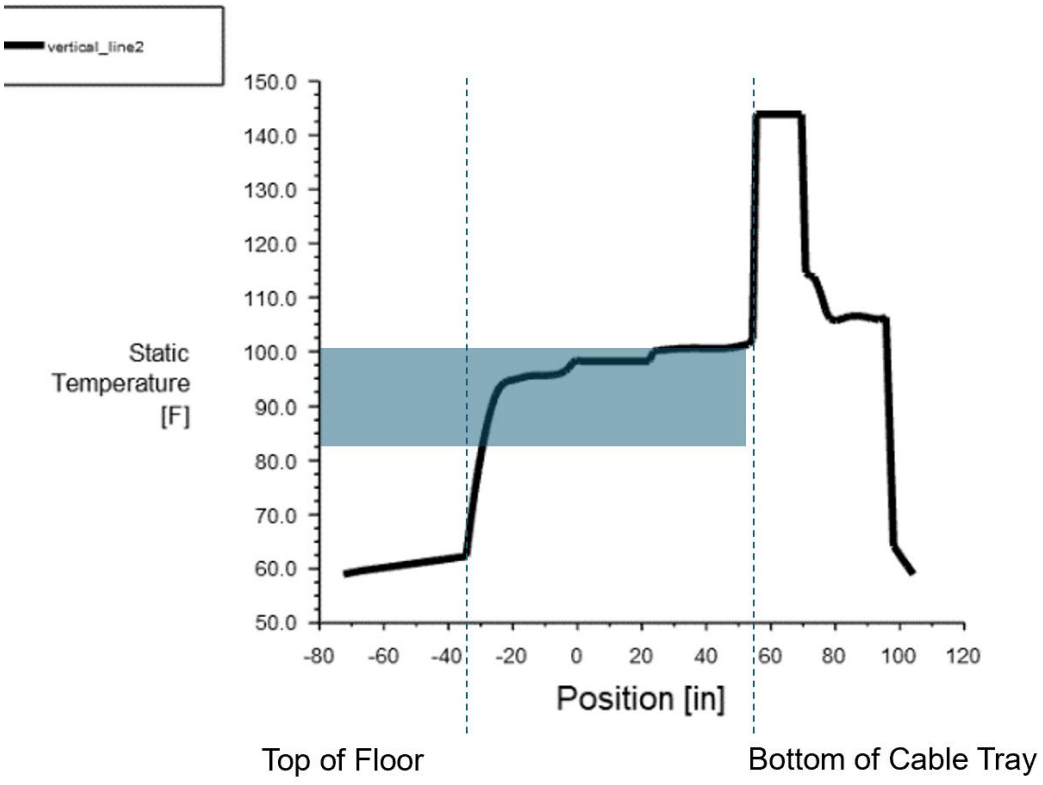


**Figure 5: Locations of tunnel floor and cable tray in temperature graph (EIC at 59°F soil Temperature)**

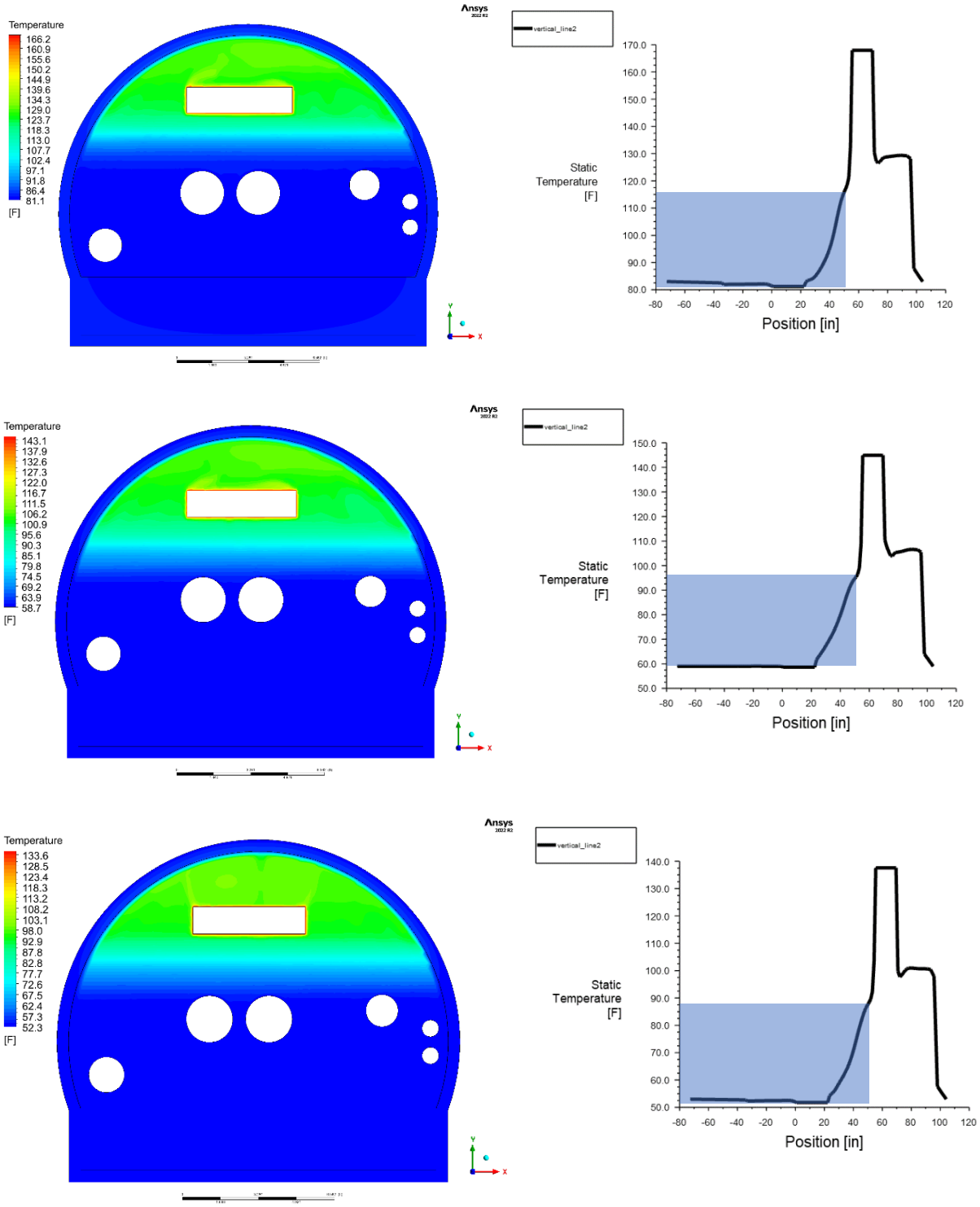


**Figure 6: RHIC Configuration at soil temperatures of 83°F (top), 59°F (middle), and 53°F (Bottom)**

Figure 7 shows the global temperature profile for the EIC configuration at the selected soil temperatures, as well as their corresponding temperature graphs of the vertical midpoint line.

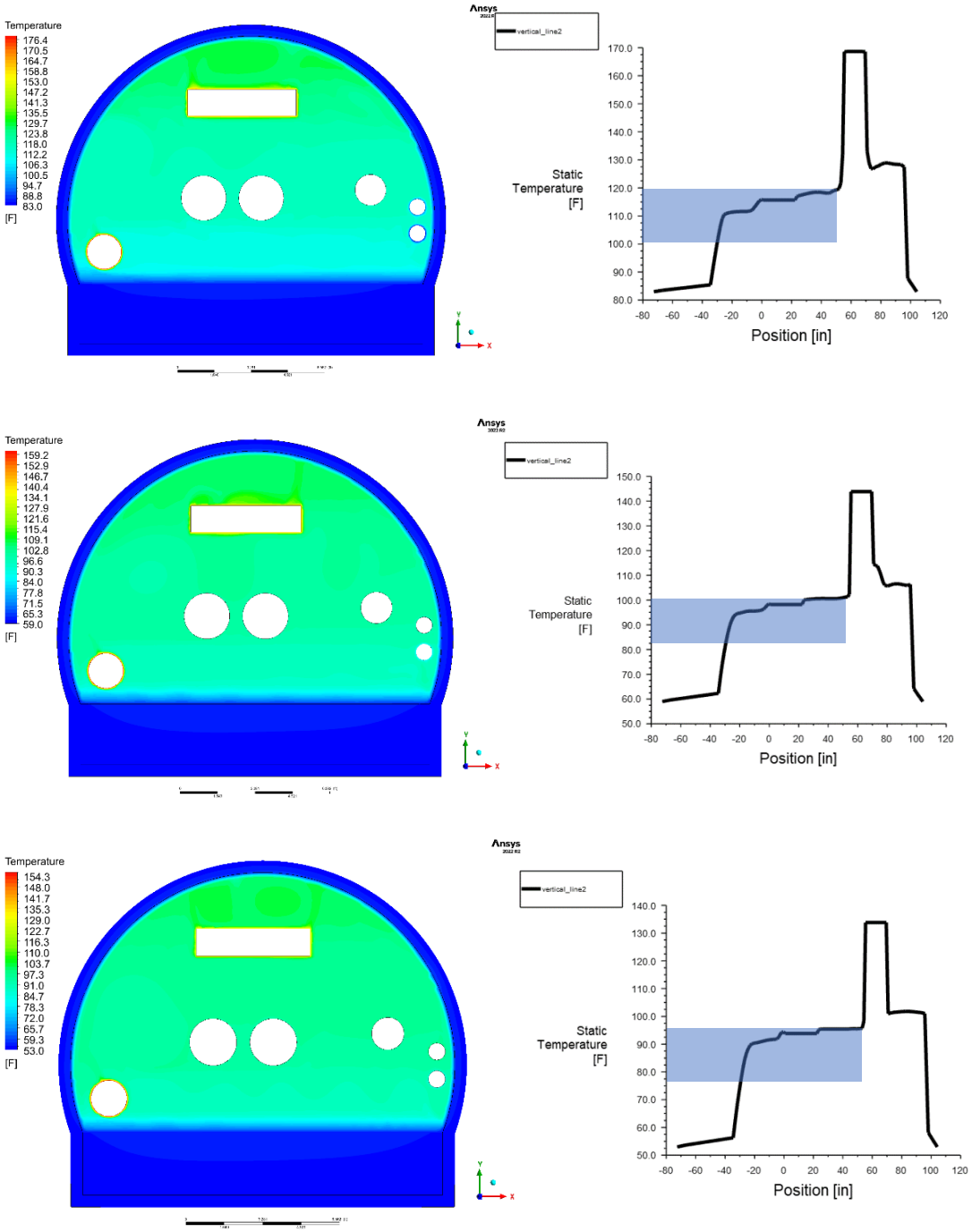


**Figure 7: EIC Configuration at soil temperatures of 83°F (top), 59°F (middle), and 53°F (Bottom)**

Figure 8 shows the global temperature profile for the EIC configuration at the selected soil temperatures when one cooling element is added to the upper left side, as well as their corresponding temperature graphs of the vertical midpoint line.

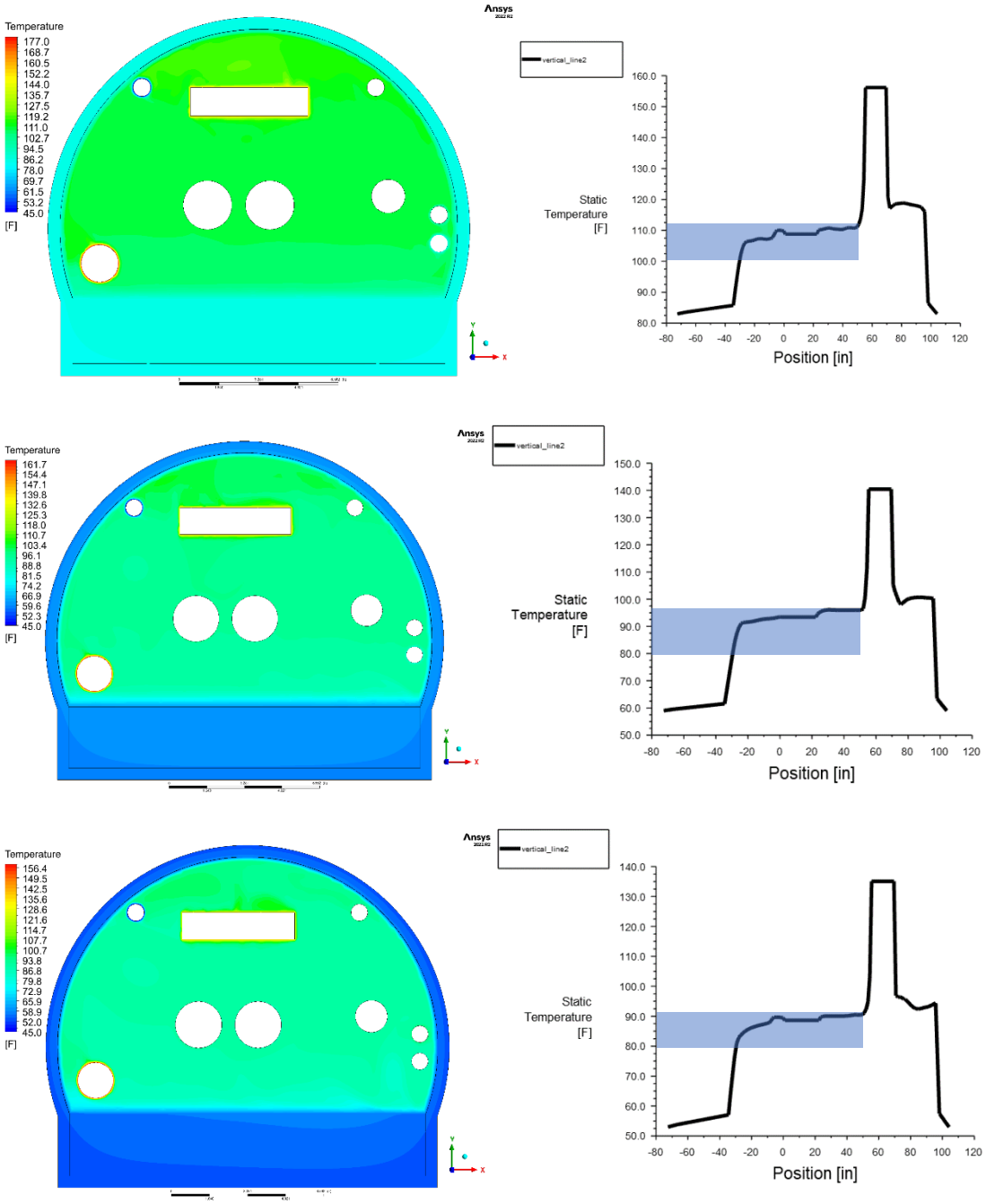


**Figure 8: EIC-1C Configuration (one cooling pipe) at soil temperatures of 83°F (top), 59°F (middle), and 53°F (Bottom)**

Figure 9 shows the global temperature profile for the EIC configuration at the selected soil temperatures when two cooling elements are added, as well as their corresponding temperature graphs of the vertical midpoint line.

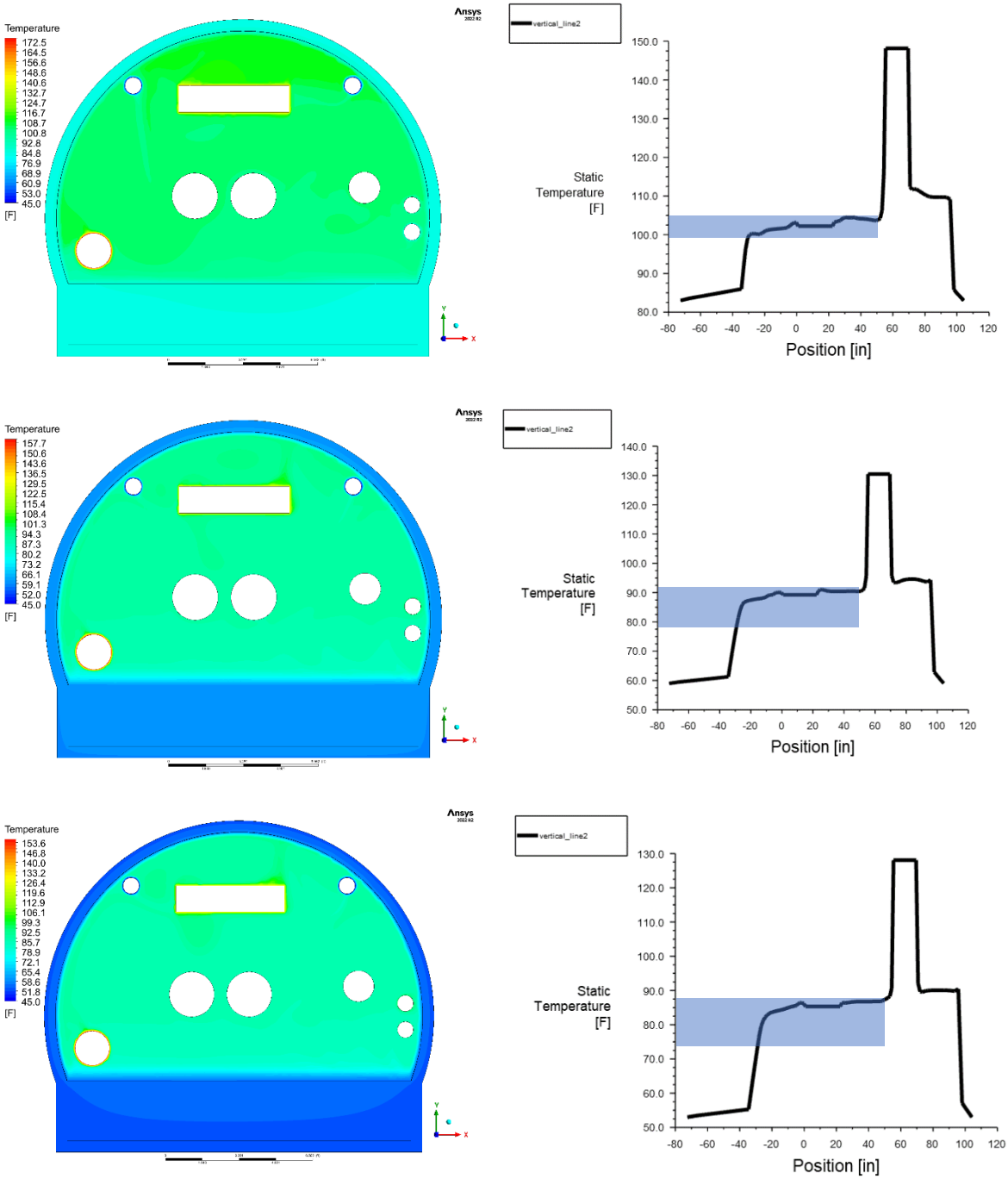


**Figure 9: EIC-2C Configuration (two cooling pipes) at soil temperatures of 83°F (top), 59°F (middle), and 53°F (Bottom)**

The temperature ranges of the area of interest for these graphs are shown in Table 3.

**Table 3: Temperature Range of Area of Interest for Model Configurations at Modeled Soil Temperatures**

| Model Configuration | Soil Temperature (°F) | Area of Interest Temperature Range (°F) |
|---|---|---|
| RHIC | 83 | 81.25 – 115 |
| | 59 | 58.75 – 95 |
| | 53 | 52.5 – 87.5 |
| EIC | 83 | 100 – 120 |
| | 59 | 82.5 – 100 |
| | 53 | 76.25 – 95 |
| EIC-1C | 83 | 100 – 112.5 |
| | 59 | 80 – 96.25 |
| | 53 | 80 – 91.25 |
| EIC-2C | 83 | 100 – 105 |
| | 59 | 77.5 – 92.5 |
| | 53 | 75 – 87.5 |

Table 3 shows that the EIC is predicted to be at a higher temperature than RHIC at all soil temperatures due to additional heating elements. At the maximum predicted soil temperature, the EIC may be as hot as 120°F within the area of interest. Adding a cooling method could lower this maximum temperature, indicating additional tunnel cooling may be valuable to EIC operations.

*Model Validation*

To access the validity of this model in predicting EIC temperatures, the results of the RHIC simulations were compared to sensor data and to data collected in the RHIC tunnels while dormant using a heat gun. The RHIC-D simulations resulted in a figure at a near-constant temperature identical to the soil temperature boundary condition and can be found in the appendix. One of the assumptions made in this model was that more minor heating components,

such as tunnel lighting, did not impact the RHIC temperature. The RHIC-D models operating under this assumption had negligible temperature differences across the tunnel profile. However, temperature data collected from the RHIC tunnel while dormant revealed a 3.1 to 6.5 °F difference in temperature between the floor and ceiling[13]. This suggests that additional heating components may play a minor role in convective heating in RHIC. The model also assumes that the soil temperature is constant all around the tunnel, despite the soil being at different depths throughout the 2D profile. If the soil temperature varies as depth increases, this may impact the profile of the tunnel temperature.

The simulations results were examined to ensure that heat transfer occurred between the fluid interior and the soil walls. Figure 10 depicts the soil walls and concrete base for RHIC and EIC models under average soil temperature conditions using a localized scale. These images show that heat does disperse through the soil walls and concrete floor, validating the model setup.

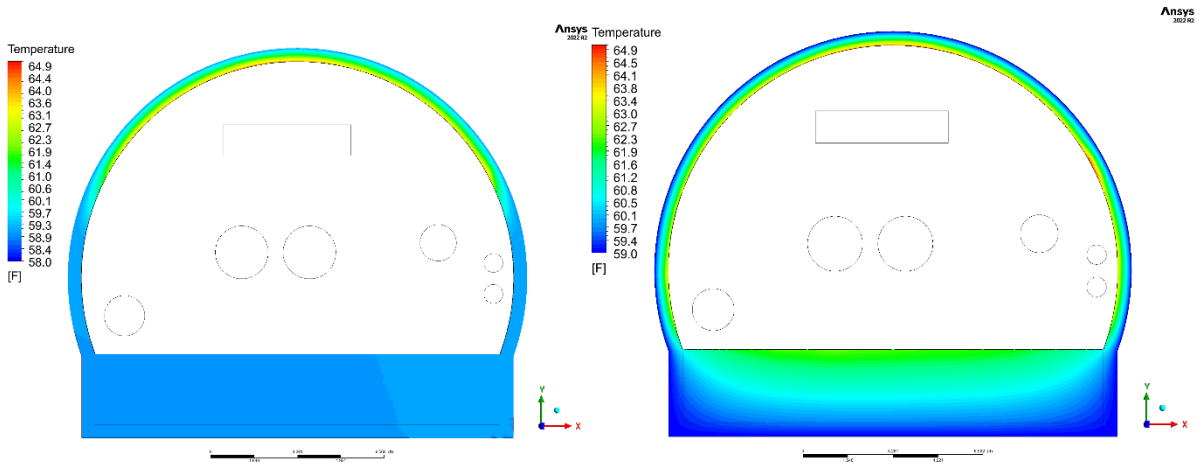


**Figure 10: Local temperature profile for the soil walls and concrete floor for RHIC (left) and EIC (right) at soil temperature of 59°F.**

One of the main factors tested for its impact on tunnel temperatures was the soil temperature, which acted as a heat sink to absorb excess heat through conduction and reduce

tunnel temperatures. To see the relationship between ambient temperature and soil temperature, both data sets were plotted, seen in Figure 11. This graph reveals that soil temperature taken six inches below sod closely follows the ambient temperature from March through October.

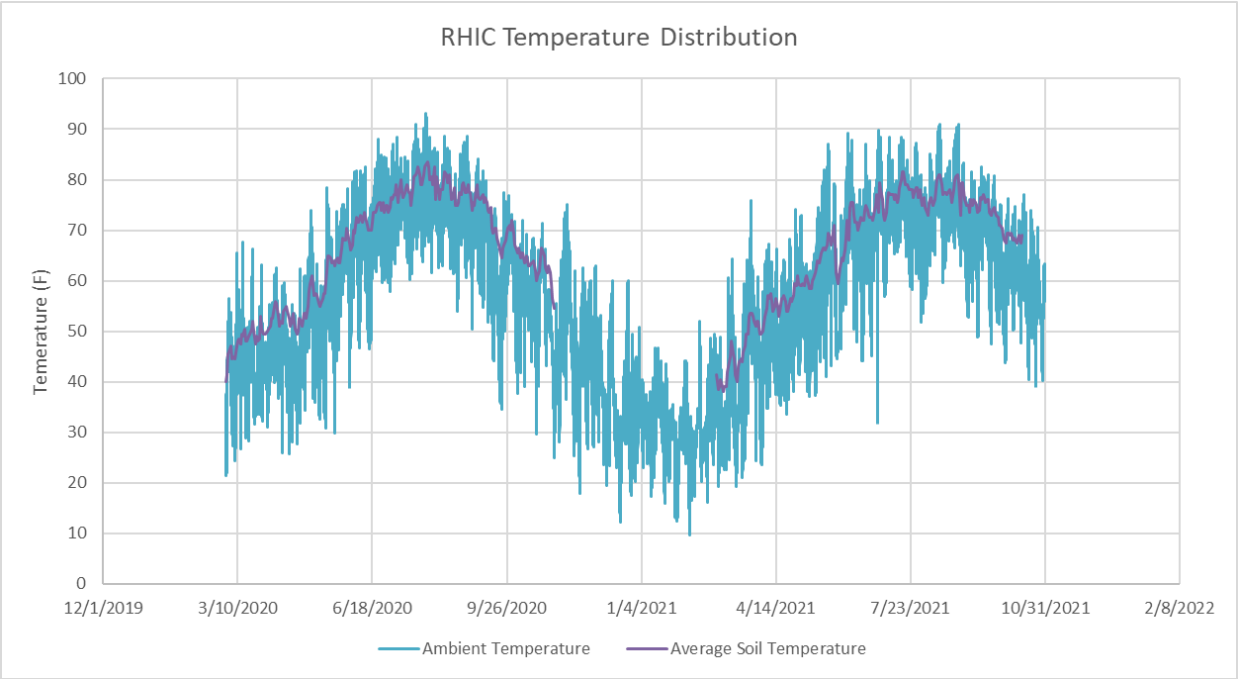


**Figure 11: Soil temperature and ambient temperature**

The relationship between the soil temperature and RHIC temperature was examined by plotting sensor data obtained from RHIC tunnel sensor B06-Q3.Q4[14] with the soil temperature and RHIC shutdown periods, as shown in Figure 12. This graph displays a lag in tunnel temperatures, shown by the phase shift in the temperature sensor data when compared to the soil temperature data. Literature shows that this lag between soil temperature and tunnel temperature commonly occurs in similar models due to a delay in tunnel heating.[15]

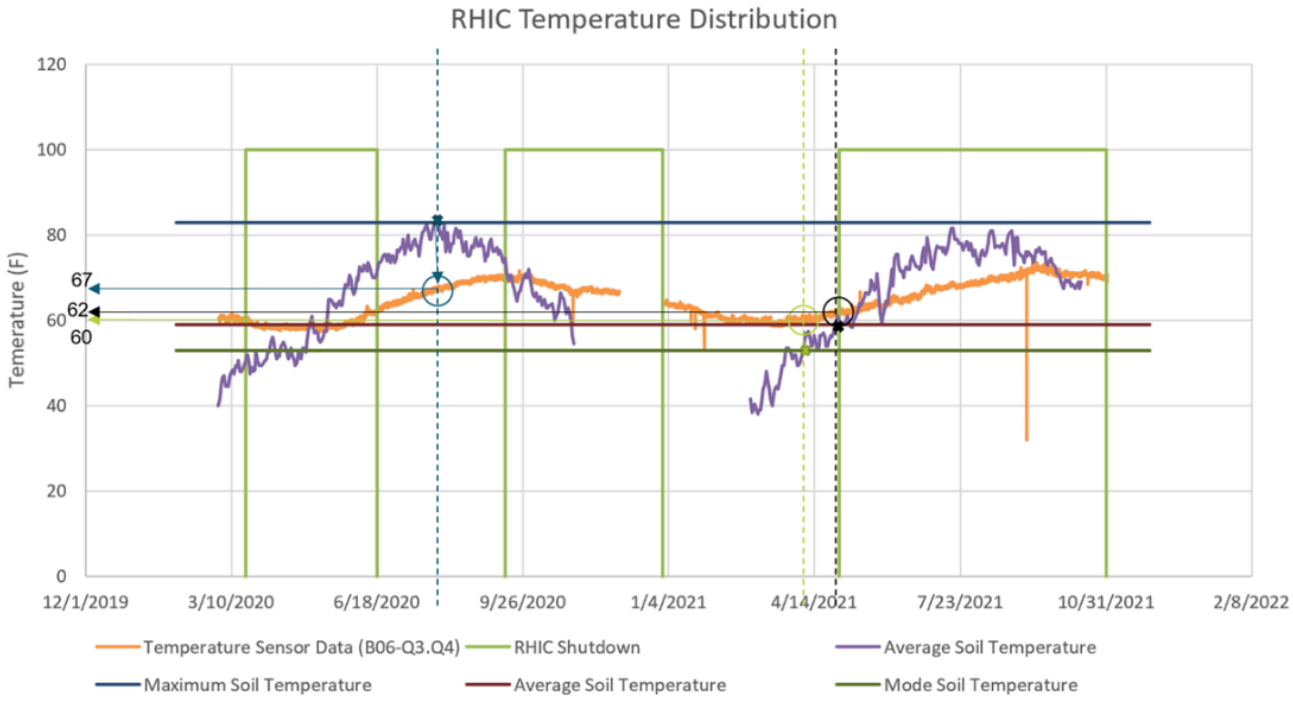


**Figure 12: Soil temperature, sensor data, and RHIC shutdown periods**

The graph shown in Figure 12 was used to determine the expected temperature of the operational RHIC model at the maximum, average, and mode soil temperatures. The approximate temperature range of the estimated sensor location in the models was then determined using the results shown in Figure 6.[16] These values are show in Table 4.

**Table 4: Expected Temperature vs Experimental Temperature**

| RHIC Soil Temperature | Expected Temperature (°F) | Experimental Temperature Range (°F) |
|---|---|---|
| Maximum (83°F) | 67 | 83-98 |
| Average (59°F) | 62 | 58-80 |
| Mode (53°F) | 60 | 51-73 |

Examining Table 4 shows that the expected temperature of RHIC fell within the experimental temperature range for the average and mode soil temperatures, but not for the maximum temperature. One possible reason for this discrepancy is that this maximum temperature is the highest of the maximum temperature data set analyzed and may be overly

conservative. Reexamining the boundary conditions and assumptions can also reveal potential causes of this unexpected outcome. One assumption that would be beneficial to reexamine is the soil temperature data. The depth of RHIC varies throughout the ring but is generally several feet deep at minimum. Literature shows that soil temperature variations decrease as soil depth increases.[17] This suggests that at a greater soil depth, the soil temperature profile shown in Figure 12 may have a smaller amplitude, which could eliminate the possibility of the maximum temperature value tested in these simulations.

## Conclusion

This project resulted in the development of a working computational fluid dynamics model that numerically solves the mass, momentum, and energy conservation equations with buoyancy effects to create a 2D temperature profile of the metal sections of the EIC tunnel. Through this model, different heat loads, temperature conditions, and configurations can be tested to determine the probable heat profile of the EIC before construction. This has the benefit of allowing for informed decision making about components and cooling systems. The current simulation shows that temperatures in the EIC for average soil conditions would be as much as 100°F. However, alterations in boundary conditions would change this prediction. As the EIC design is altered and as new soil data is analyzed, the model can be updated to match new conditions. Further steps that can be taken to improve the model include an investigation into the relationship between soil temperature and soil depth to ensure accurate soil temperature data. Creating a 3D model that can account for additonal convective forces in the tunnel would be beneficial as it would model natural convection with more complexity and allow for the examination of more sophisticated cooling systems. This model is the first step in predicting the

temperature distribution of the EIC, and will positively impact the cost and schedule of the infrastructure descisions of this accelerator-collider as it continues to evolve.

**Acknowledgements**

This project was supported in part by the U.S. Department of Energy, Office of Science, Office of Workforce Development for Teachers and Scientists (WDTS) under the Science Undergraduate Laboratory Internships Program (SULI). I'd also like to thank Ram Srinivasan, the EIC Infrastructure Department, Logan Norman, and Skylar Polek.

**References**

[1]Pimenta dos Santos, M. A. "Thermal Analysis of One LHC Tunnel Octant." *European Organization for Nuclear Research: CERN - ST Division*, 19 June 2000, pp. 1–20.

[2]*Electron-Ion Collider: Relativistic Heavy Ion Collider (RHIC) Buried Tunnel Structural Integrity Inspection Report.* Brookhaven National Laboratory, Dec. 2021, p. 3-6

[3]"a3001906-4," AutoCAD Tunnel Drawings, Brookhaven National Laboratory. Infrastructure Division>EIC Utility Requirements Interface>Utilities Requirements by Group>Water Activation Potential>Tunnel Drawings

[4]"dsh_bnl_eic_ir10_build-up.stp" March 31, 2022, 32.6mb, Brookhaven National Laboratory.

[5]Sun, Tingting, et al. "An Analytical Model to Predict the Temperature in Subway-Tunnels by Coupling Thermal Mass and Ventilation." *Journal of Building Engineering*, vol. 44, 10 May 2021, p. 102564, 10.1016/j.jobe.2021.102564. Accessed 20 July 2022.

[6]Krarti, Moncef, and Jan F. Kreider. “Analytical Model for Heat Transfer in an Underground Air Tunnel.” *Energy Conversion and Management*, vol. 37, no. 10, 9 July 1995, pp. 1561–1574. *Elsevier*, 0196-8904(95)00208-1.

[7]“MAGNETS Infrastructure Utility Requirements April 2022.” July 20, 2022. 774 kb. Infrastructure Division>EIC Utility Requirements Interface>Utilities Requirements by Group>Magnet>MAGNETS Infrastructure Utility Requirements April 2022.xlsx

[8]Norman, Logan. “Computational fluid dynamic modeling to determine the indoor environment of an electron-ion collider service building.” Office of Educational Programs, 2022 Compilation of Internship Reports, Brookhaven National Laboratory, https://www.bnl.gov/education/resources.php

[9]Than, Roberto. “Re: Cryo Pipe Temperature In the Tunnel.” Received by Ram Srinivasan, 27 July 2022. Email Interview.

[10]Vultaggio, Sandra. “Soil Growing Degree Days (GDD) (50° F.) – 2021,” *Cornell Cooperative Extension - Suffolk County*

[11]Çengel Yunus A, and Afshin J Ghajar. *Heat and Mass Transfer: Fundamentals & Applications, Fourth Edition*. New York, Ny, McGraw-Hill, 2011, p. 904.

[12]“Meteorology Services - Data Downloads.” *Brookhaven National Laboratory Meteorological Services*, wx1.bnl.gov/download.htm. Accessed 20 July 2022.

[13]Letourneau, Emma. “Data Collection and Constant Values.” 32 kb, July 2022, Infrastructure Division>Interns>Summer 2022>Project Work

[14]Thomas, Dillon. “From Dillon Thomas via teams on 7-15-21 rhictemphumidions,” *Brookhaven National Laboratory*

[15]Stefan, Sadokierski, and Thiffeault Jean-Luc. “Heat Transfer in Underground Rail Tunnels.” *Elsevier Science,* 26 Oct. 2018, pp. 1–31.

[16] An estimated sensor location range was used instead of a precise location because the exact location of the sensor on the 2D model was not known, so the most porbable range was determined to be slightly above the tunnel floor to midway between the cable tray and the Hadron beams.

[17]Ochsner, Tyson. “13.4 Sub-Surface Soil Temperatures.” *Open.library.okstate.edu*, 17 June 2019, open.library.okstate.edu/rainorshine/chapter/13-4-sub-surface-soil-temperatures/. Accessed 9 Aug. 2022.

## Appendix

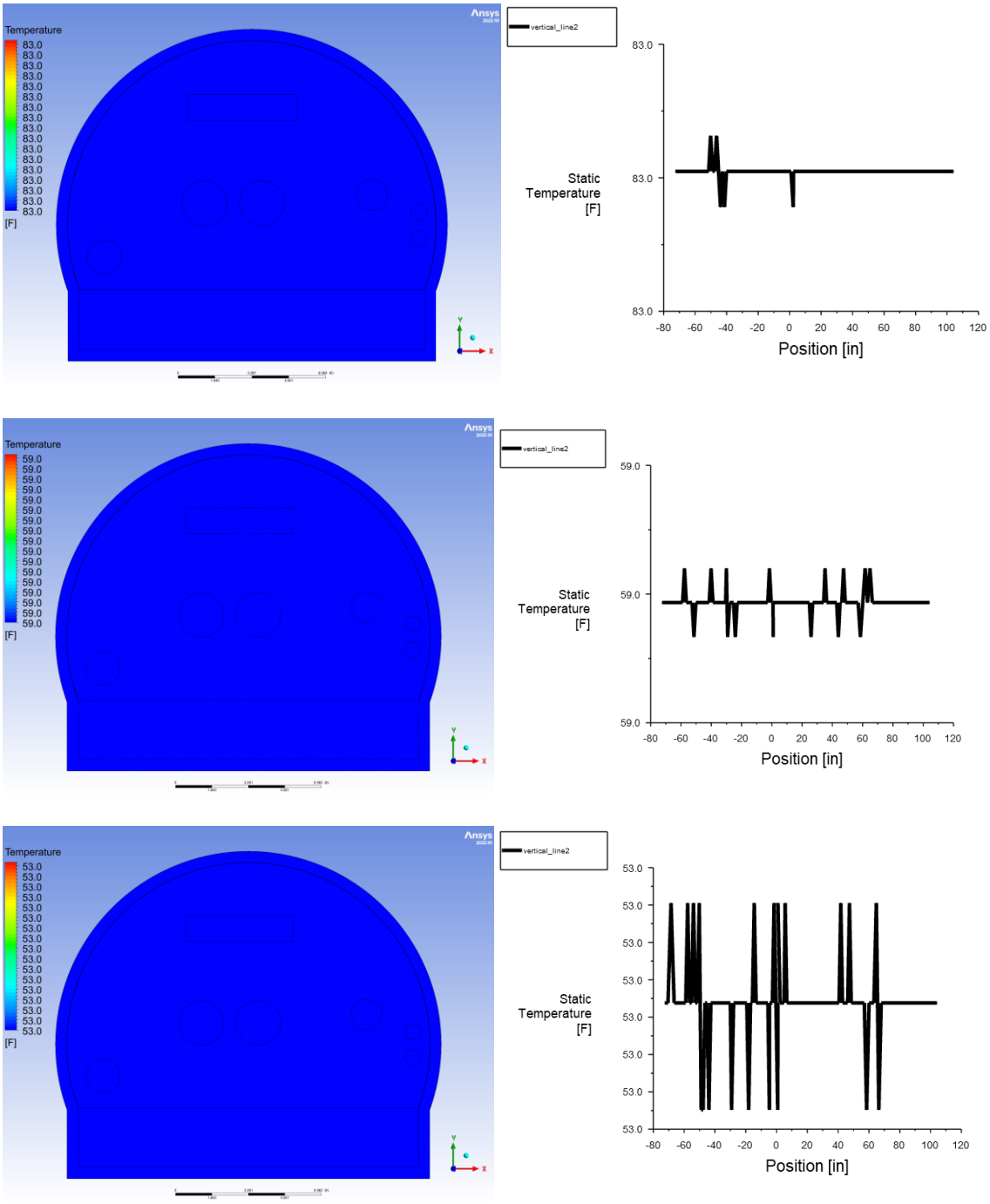


**Figure 13: RHIC-D Configuration at soil temperatures of 83°F (top), 59°F (middle), and 53°F (Bottom)**

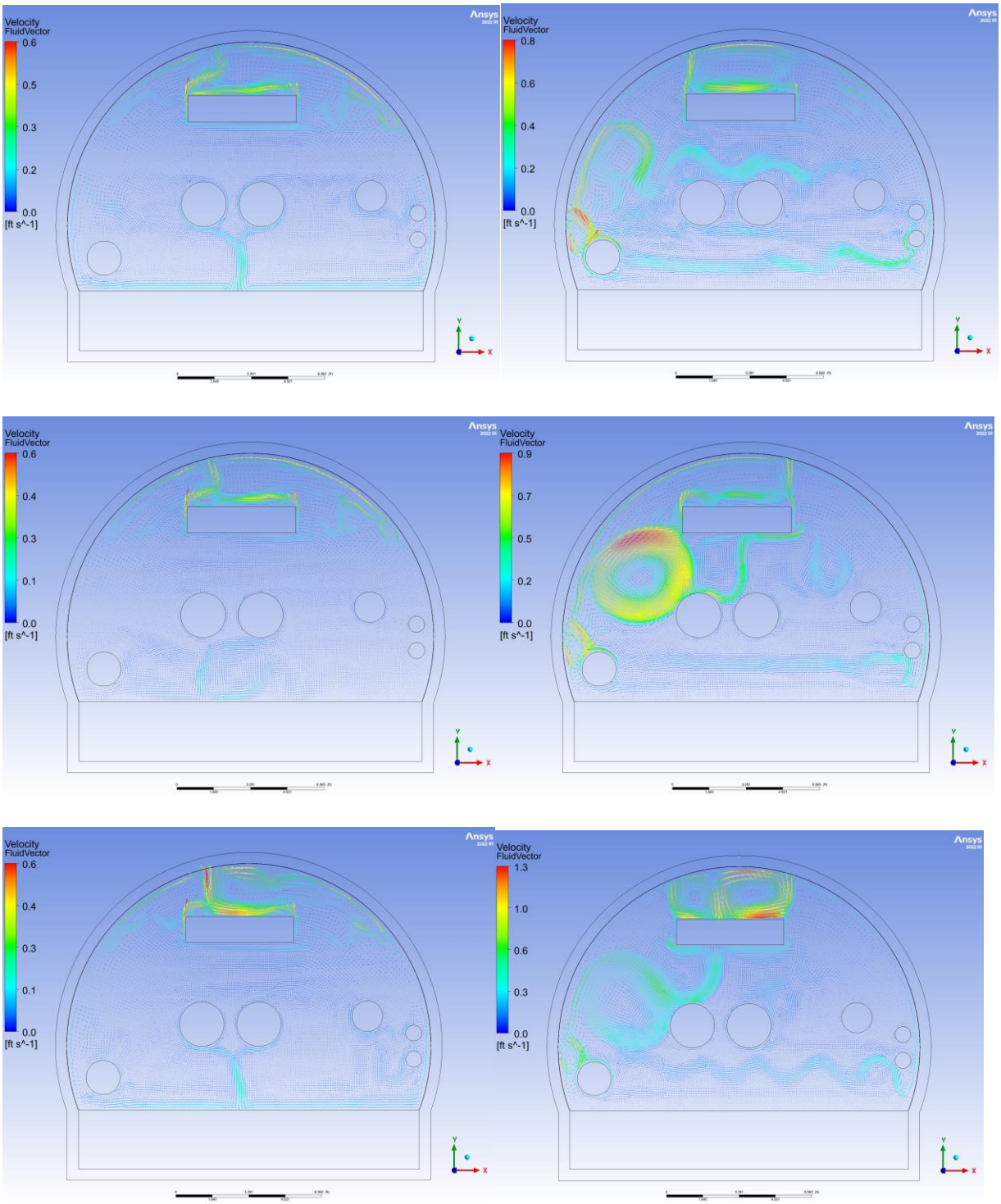


**Figure 14: Velocity Vectors of RHIC Configuration (left) EIC Configuration (right) at soil temperatures of 83°F (top), 59°F (middle), and 53°F (Bottom)**